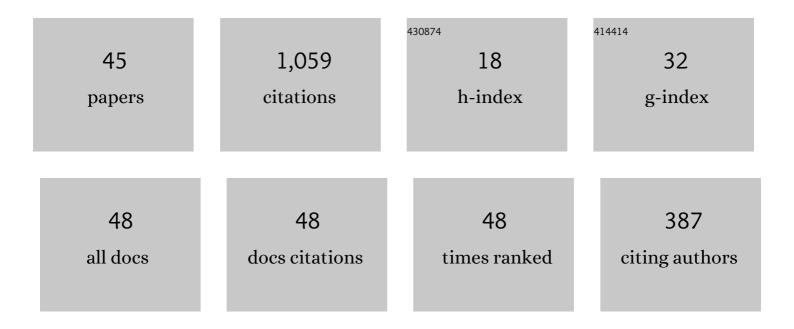
## John M Harlander

List of Publications by Year in descending order

Source: https://exaly.com/author-pdf/2694345/publications.pdf Version: 2024-02-01



ΙΟΗΝ ΜΗΛΡΙΑΝΠΕΡ

#	Article	IF	CITATIONS
1	Michelson Interferometer for Global High-Resolution Thermospheric Imaging (MIGHTI): Instrument Design and Calibration. Space Science Reviews, 2017, 212, 553-584.	8.1	116
2	Doppler asymmetric spatial heterodyne spectroscopy (DASH): concept and experimental demonstration. Applied Optics, 2007, 46, 7297.	2.1	92
3	Shimmer: a spatial heterodyne spectrometer for remote sensing of Earth' middle atmosphere. Applied Optics, 2002, 41, 1343.	2.1	90
4	The MIGHTI Wind Retrieval Algorithm: Description and Verification. Space Science Reviews, 2017, 212, 585-600.	8.1	74
5	Robust monolithic ultraviolet interferometer for the SHIMMER instrument on STPSat-1. Applied Optics, 2003, 42, 2829.	2.1	56
6	Correction of phase distortion in spatial heterodyne spectroscopy. Applied Optics, 2004, 43, 6680.	2.1	56
7	Design and laboratory tests of a Doppler Asymmetric Spatial Heterodyne (DASH) interferometer for upper atmospheric wind and temperature observations. Optics Express, 2010, 18, 26430.	3.4	48
8	Validation of ICONâ€MIGHTI Thermospheric Wind Observations: 2. Greenâ€Line Comparisons to Specular Meteor Radars. Journal of Geophysical Research: Space Physics, 2021, 126, e2020JA028947.	2.4	45
9	Initial ground-based thermospheric wind measurements using Doppler asymmetric spatial heterodyne spectroscopy (DASH). Optics Express, 2010, 18, 27416.	3.4	43
10	Validation of ICONâ€MIGHTI Thermospheric Wind Observations: 1. Nighttime Red‣ine Groundâ€Based Fabryâ€Perot Interferometers. Journal of Geophysical Research: Space Physics, 2021, 126, e2020JA028726.	2.4	43
11	Spatial Heterodyne Imager for Mesospheric Radicals on STPSatâ€1. Journal of Geophysical Research, 2010, 115, .	3.3	41
12	Michelson Interferometer for Global High-Resolution Thermospheric Imaging (MIGHTI): Monolithic Interferometer Design and Test. Space Science Reviews, 2017, 212, 601-613.	8.1	40
13	Broadband, high-resolution spatial heterodyne spectrometer. Applied Optics, 2008, 47, 6371.	2.1	30
14	Spatial heterodyne spectroscopy: interferometric performance at any wavelength without scanning. , 1990, , .		26
15	Retrieval of Lower Thermospheric Temperatures from O2 A Band Emission: The MIGHTI Experiment on ICON. Space Science Reviews, 2018, 214, 1.	8.1	26
16	Spatial heterodyne spectroscopy at the Naval Research Laboratory. Applied Optics, 2015, 54, F158.	2.1	25
17	Regulation of ionospheric plasma velocities by thermospheric winds. Nature Geoscience, 2021, 14, 893-898.	12.9	25
18	First results from the Spatial Heterodyne Imager for Mesospheric Radicals (SHIMMER): Diurnal variation of mesospheric hydroxyl. Geophysical Research Letters, 2008, 35, .	4.0	24

JOHN M HARLANDER

#	Article	IF	CITATIONS
19	First results from an all-reflection spatial heterodyne spectrometer with broad spectral coverage. Optics Express, 2010, 18, 6205.	3.4	20
20	High-efficiency echelle gratings for MICHTI, the spatial heterodyne interferometers for the ICON mission. Applied Optics, 2017, 56, 2090.	2.1	17
21	Vertical Coupling by Solar Semidiurnal Tides in the Thermosphere From ICON/MIGHTI Measurements. Journal of Geophysical Research: Space Physics, 2022, 127, .	2.4	16
22	Atmosphereâ€lonosphere (Aâ€l) Coupling as Viewed by ICON: Dayâ€toâ€Day Variability Due to Planetary Wave (PW)â€Tide Interactions. Journal of Geophysical Research: Space Physics, 2021, 126, e2020JA028927.	2.4	14
23	Thermal sensitivity of DASH interferometers: the role of thermal effects during the calibration of an Echelle DASH interferometer. Applied Optics, 2013, 52, 8082.	1.8	13
24	Quasiâ€2â€Day Wave in Lowâ€Latitude Atmospheric Winds as Viewed From the Ground and Space During January–March, 2020. Geophysical Research Letters, 2021, 48, e2021GL093466.	4.0	13
25	Errors From Asymmetric Emission Rate in Spaceborne, Limb Sounding Doppler Interferometry: A Correction Algorithm With Application to ICON/MIGHTI. Earth and Space Science, 2020, 7, e2020EA001164.	2.6	11
26	Flat-fields in DASH interferometry. Optics Express, 2012, 20, 9535.	3.4	10
27	Vertical Shears of Horizontal Winds in the Lower Thermosphere Observed by ICON. Geophysical Research Letters, 2022, 49, .	4.0	9
28	On the uncertainties in determining fringe phase in Doppler asymmetric spatial heterodyne spectroscopy. Applied Optics, 2019, 58, 3613.	1.8	7
29	Laboratory demonstration of mini-MIGHTI: A prototype sensor for thermospheric red-line (630Ânm) neutral wind measurements from a 6U CubeSat. Journal of Atmospheric and Solar-Terrestrial Physics, 2020, 207, 105363.	1.6	6
30	Calibration lamp design, characterization, and implementation for the Michelson Interferometer for Global High-Resolution Thermospheric Imaging instrument on the Ionospheric Connection satellite. Optical Engineering, 2019, 58, 1.	1.0	5
31	Determining the thermomechanical image shift for the MIGHTI instrument on the NASA-ICON satellite. Optical Engineering, 2020, 59, 1.	1.0	5
32	High sensitivity trace gas sensor for planetary atmospheres: miniaturized Mars methane monitor. Journal of Applied Remote Sensing, 2014, 8, 083625.	1.3	4
33	Q2DWâ€ŧide and â€ionosphere interactions as observed from ICON and groundâ€based radars. Journal of Geophysical Research: Space Physics, 2021, 126, e2021JA029961.	2.4	4
34	The Field-Widened SHS: An Extremely High etendue, Unscanned, Michelson-Based Spectrometer. International Astronomical Union Colloquium, 1995, 149, 336-337.	0.1	2
35	Measurement and modeling of the thermal behavior of a laboratory DASH interferometer. Proceedings of SPIE, 2012, , .	0.8	1
36	Mini-Mighti: A Prototype Sensor For Thermospheric Red-Line (630 Nm) Neutral Wind Measurements From A 6u Cubesat. , 2019, , .		1

JOHN M HARLANDER

#	Article	IF	CITATIONS
37	Compression Assembly of Spatial Heterodyne Spectroscopy Interferometers. Recent Patents on Space Technology, 2011, 1, 1-6.	0.1	0
38	The As-Built Performance of the MIGHTI Interferometers. , 2016, , .		0
39	Determining the thermomechanical image shift for the MIGHTI instrument on the NASA-ICON satellite (Erratum). Optical Engineering, 2021, 60, .	1.0	0
40	Doppler Asymmetric Spatial Heterodyne (DASH) Interferometer from Flight Concept to Field Campaign. , 2011, , .		0
41	Laboratory and field tests of a Doppler Asymmetric Spatial Heterodyne (DASH) spectrometer for thermospheric wind observations. , 2011, , .		0
42	Design and Laboratory Tests of the Michelson Interferometer for Global High-resolution Thermospheric Imaging (MIGHTI) on the Ionospheric Connection Explorer (ICON) Satellite. , 2015, , .		0
43	An Overview of Design Challenges and the Data Analysis Approach of the Thermospheric Wind and Temperature Instrument on the NASA ICON Mission. , 2018, , .		0
44	An Overview of Design Challenges and the Data Analysis Approach of the Thermospheric Wind and Temperature Instrument on the NASA ICON Mission. , 2019, , .		0
45	On-orbit Performance of the Thermospheric Wind and Temperature Instrument on the NASA ICON Mission. , 2021, , .		0